Cement and Concrete Research 42 (2012) 148–157

Contents lists available at SciVerse ScienceDirect

Cement and Concrete Research

journal homepage: http://ees.elsevier.com/CEMCON/default.asp

The origins of thixotropy of fresh cement pastes

N. Roussel [a,*], G. Ovarlez [b], S. Garrault [c], C. Brumaud [a]

[a] Université Paris Est, IFSTTAR, France
[b] Université Paris Est, Laboratoire Navier (UMR CNRS), France
[c] ICB, UMR/CNRS 5209, France

ARTICLE INFO

Article history:
Received 6 September 2010
Accepted 14 September 2011

Keywords:
Thixotropy
Rheology (A)
Hydration (A)

ABSTRACT

In this paper, we show that the thixotropic behavior of standard fresh cement pastes may find two origins. We first clarify the ambiguity in literature concerning the critical strain of fresh cement pastes, thanks to a detailed analysis of their macroscopic behavior. We show that the largest critical strain can be associated to the network of colloidal interactions between cement particles whereas the smallest critical strain can be associated to the early hydrates, which form preferentially at the contact points between cement grains. From the study of the structuration kinetics, we show that there exists a short term thixotropy due to colloidal flocculation along with a long term thixotropy (of practical interest) due to the ongoing hydrates nucleation. From dimensional considerations, we moreover suggest why the apparent yield stress of the mixture left at rest can be approximated as a linear function of time.

1. Introduction

The vast majority of cementitious materials are able to support a finite amount of stress without flowing. Macroscopic flow is however achieved as soon as the stress applied to the system overcomes what can be supported by the network of particles in interaction. This critical value is called yield stress and is the dominant intrinsic parameter of what is called in practice workability of concrete [1,2].

In many cementitious materials, a reversible evolution of the material rheological behavior is often noted during the so-called dormant period of the hydration reaction: at rest, the apparent yield stress (or static yield stress) continuously increases [1–9]. As this evolution can be erased by a strong shearing or remixing of the paste and the material can be brought back to a reference state, it is often described as thixotropy. The origin of this evolution is however very unclear. The word "structuration" is therefore often used to describe the consequences of this thixotropic behavior as this word is not associated to a specific physical phenomenon [8,9]. It only implies that a structure is being built or destroyed within the material all along its flow history. As this structural evolution is macroscopically reversible, most explanations available in literature focus on microscopic reversible physical phenomena, such as reversible colloidal flocculation and deflocculation. Very various phenomena can however be at the origin of thixotropy for other materials in nature or industry. Of course, reversible colloidal flocculation may explain thixotropy in many suspensions but reversible entanglement of polymer chains or reversible orientation of Brownian slender particles is also a potential explanation for macroscopic thixotropic behavior [3].

Yield stress is dictated by the structure and strength of the network of cement particles in interaction [10,11]. Accumulated experimental and numerical evidence show that network rupture in particle suspension occurs when its initial structure has been sufficiently modified, namely for a critical strain γ_c [12–14]. This critical strain and the yield stress should then be related by $\tau_0 = G\gamma_c$ where G is the shear elastic modulus as long as we assume a linear elastic behavior in the solid regime below the yield stress.

There is however a strong ambiguity in the literature concerning the value of the critical strain of cement pastes. When Mahaut et al. [15] or Schmidt and Schlegel [16] study the transition from rest to flow (Fig. 1), they measure a critical strain of the order of several % while other studies using oscillary rheometry (Fig. 1) point towards values of the order of few hundredths of % [17,18]. A better understanding of the mechanisms of yielding, which is crucial for the understanding of the origin of thixotropy, implies that this ambiguity has to be understood.

Let us first note that, in the above four papers, what is called "flow onset" or "critical strain" strongly differs. In the first case [15,16], flow onset is associated to strong structural changes in the material. During this type of experiments, a shear stress is measured as a function of time while applying a low constant strain rate. The rheological tools can be parallel plates, coaxial cylinders or Vane test. Only the peak in the shear stress curve in Fig. 1 (left) is considered as it is when the applied stress is higher than this peak value that the material flows in terms of practical applications. This value is called apparent or static yield stress [9,19]. For example, in the case of shotcrete, it is this critical value that will control if the material stays on the wall

* Corresponding author. Tel.: +33 140435285.
E-mail address: nicolas.roussel@lcpc.fr (N. Roussel).

0008-8846/$ – see front matter © 2011 Elsevier Ltd. All rights reserved.
doi:10.1016/j.cemconres.2011.09.004

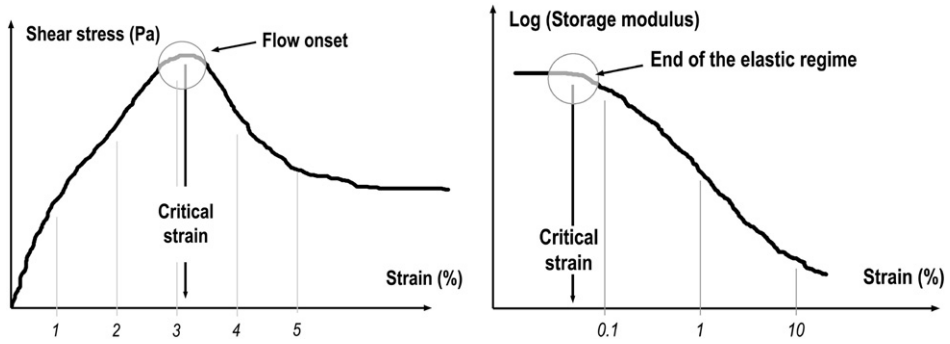

Fig. 1. The two critical strains in literature (sketch). (Left): critical strain of the order of a few % in a yield stress measurement; (right): critical strain of the order of a few hundredths of % in a storage (or elastic) shear modulus measurement.

in thick layers rather than flow down. When this type of measurement is carried out on concrete, mortar or cement paste after a resting time no longer than a few minutes, the critical strain associated to the peak value is usually of the order of a few %.

In the second case [17,18], the measured critical strain is associated to the end of the linear elastic regime. Strain oscillations of increasing amplitudes are applied to the tested material. The frequency of the oscillation is of the order of 1 Hz and the elastic shear modulus of the material is computed from the measured stress [17,18]. The critical strain is defined by the onset of an important decrease of shear modulus as shown in Fig. 1 (right) and not, as above, by a true measurement of the flow onset. As flow in simpler materials, like model colloidal suspensions [20], corresponds to the end of the elastic regime, this is a natural way to measure a critical strain. For many materials in nature or industry, both definitions and measurement protocols then lead to a more or less identical value of the critical strain [20–22]. The discrepancies between both values in the case of cement pastes would then mean that, at the smallest critical strain, the system does not really begin to flow and does not experience any reorganization of the cement particle network.

The aim of the first part of this paper is to understand the difference between the two critical strains described above, and to show how the mechanisms at the origin of this difference affect yield stress and thixotropy. We first show that, in fact, there does not exist only one but at least two critical strains in fresh cement pastes. Our observations suggest that the largest critical strain can be associated to the breakage of the network of colloidal interactions between cement particles, which forms shortly after the end of mixing, and that the smallest critical strain can be associated to the breakage of the early hydrates, which form preferentially at the contact points between flocculated cement grains.

In the second part of this paper, from the study of the structuration kinetics of the macroscopic properties (elastic modulus, yield stress) associated with these two strain scales, we suggest that there exists a short term thixotropy due to colloidal flocculation with a characteristic time of the order of a few seconds along with a long term thixotropy (of practical interest) due to the ongoing hydrates nucleation. From a simple dimensional micromechanical approach, we moreover explain why apparent or static yield stress of the mixture left at rest can be approximated, in most cases, as a linear function of time.

2. Origin of the two critical strains of fresh cement pastes

In order to clarify the ambiguity about the critical strain in literature, we first study the macroscopic behavior of a pure cement paste (*i.e.* no organic or mineral admixtures) during both yield stress measurement and elasticity measurement. We focus on both small and large strains and compare the information that can be obtained from both techniques.

2.1. Experimental measurements

We plot in Fig. 2 the results of a Vane test experiment on a cement paste (water to cement weight ratio W/C = 0.4). The cement is a CEM I from Lafarge, Le Havre, France. The measurements are carried out using a *C-VOR Bohlin*® rheometer. The Vane geometry is a four-bladed paddle with a diameter of 25 mm, the outer cup diameter is 50 mm and its depth is 60 mm. 20 min after the end of the mixing phase, the cup of the rheometer is filled and the sample is sheared at 150 s^{-1} for 200 s. After a 5 minute resting time, a constant shear rate of 0.005 s^{-1} is applied to the sample. After an initial increase of the shear stress, the stress peak is followed by a plateau representative of steady state flow. The main feature in Fig. 2(a) is the flow start for a critical shear strain equal to 2.5%. The associated static or apparent yield stress (*i.e.* the stress peak) is of the order of 32 Pa whereas the stress at the plateau is of the order of 27 Pa.

If we now zoom on the first few tenths of % strain in Fig. 2(b), we can however spot another feature, far less visible than the first one when using standard linear scales. In the very first stages of the shearing process, the shear stress first increases very rapidly with the shear strain: this would correspond to the behavior of a very stiff material. Then, for a critical shear strain of the order of 0.05%, there is an abrupt change of the stress/strain slope: the shear stress starts increasing very smoothly with the shear strain, which corresponds to what is usually observed as in Fig. 2(a). It can then be noted that the instantaneous (or apparent) shear modulus (*i.e.* the ratio between shear stress and shear strain) for strains lower than a few hundredths of % is of the order of several thousands of Pa whereas it is of the order of several hundreds of Pa at the stress peak.

The shear storage modulus G' is usually measured in oscillation experiments. The classical experiment then consists in applying strain oscillations and in measuring the stress response.

As elastic effects are in phase with the strain whereas viscous effects are in phase with the strain rate (and thus in quadrature with the strain), this defines an elastic modulus G' and a viscous modulus G''. It is also possible to define a complex modulus $G^* = G' + \mathbf{i}G''$. When viscous effects can be neglected (*i.e.* low shear rates or solid behavior), G' should be of the same order of magnitude as the instantaneous (or apparent) shear modulus, which is defined as the instantaneous ratio between shear stress and shear strain during a yield stress measurement such as the one in Fig. 2. We compare in Fig. 3 these two *moduli* in the case of the same cement paste as in the above section. The instantaneous shear modulus is calculated from the above Vane test result at 0.005 s^{-1} by dividing the measured shear stress by the shear strain whereas the shear storage modulus G' is measured at an oscillation frequency of 1 Hz as a function of the strain amplitude between 0.001% and 1%. In both cases, the Vane tool described above is used. 20 min after the end of mixing, the material is pre-sheared at 150 s^{-1} for 200 s before the measurement. The test starts after a five minute resting time.

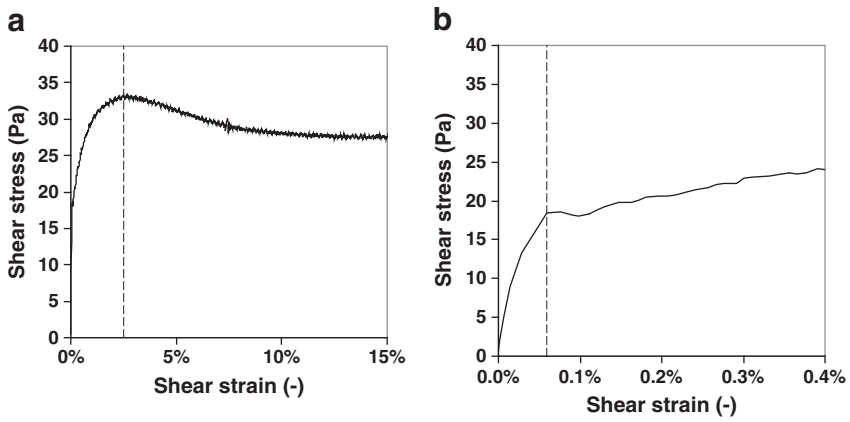

Fig. 2. Shear stress as a function of shear strain during a Vane test on a cement paste with a water to cement ratio of 0.4. (a) Linear shear strain scale from 0 to 15%; (b) Linear shear strain scale from 0 to 0.4%.

We see in Fig. 3 that, below a few hundredths of % of strain, both storage and instantaneous shear *moduli* are roughly constant defining an elastic linear regime. The brutal drop in instantaneous shear modulus in Fig. 2(b) can therefore be associated to the critical strain defined as the end of the linear elastic regime in Ref. [17]. We also see that, below a few % both *moduli* have the same order of magnitude while, from Fig. 2(a), we know that flow has not started yet in the material: this means that, in contrast with simple yield stress fluids [20–22], the strong decrease in the elastic modulus of cement pastes with strain cannot be interpreted directly as a signature of yielding.

To summarize, we see that looking at both standard yield stress measurement and elastic modulus measurement provides a macroscopic description of two critical strains of cement pastes, which both exist simultaneously. The first critical strain is clearly associated with a very stiff elastic behavior of the material at low strain, while the second critical strain is associated with yielding and flow onset. The following section is devoted to the discussion of the microscopic origin of these critical strains. It may be useful to keep in mind at this stage that a critical strain as defined here is associated to an important change in the mechanical properties. Although the stress needed to reach this critical strain may result from the contribution of various phenomena, the value of the critical strain provides a strong signature of the dominant phenomenon *e.g.*, rigid and fragile materials have low fracture critical strains whereas organic polymer based materials, for instance, often display critical strains which are order of magnitudes larger.

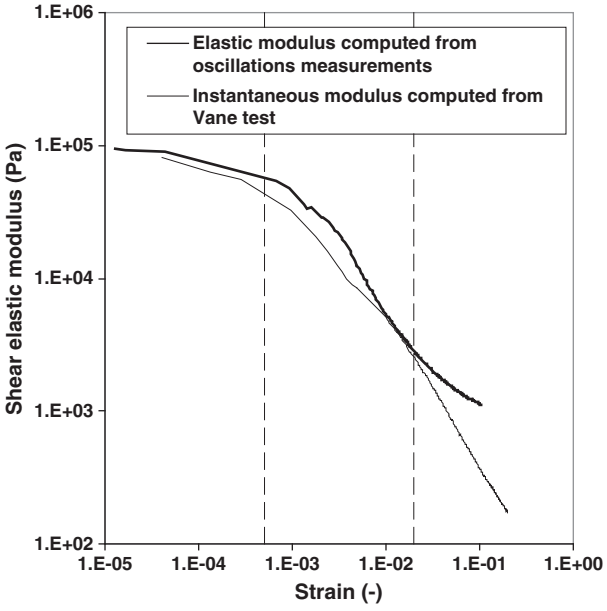

Fig. 3. Shear elastic modulus as a function of strain. The oscillation frequency is 1 Hz and the strain amplitude is increased from 1.10^{-5} to 1.10^{-1}. The shear rate is 0.005 s^{-1} for the Vane test. The two dashed vertical lines correspond to the two critical shear strains.

2.2. The smallest critical strain: the CSH contribution

To understand the origin of the first critical strain, let us first comment its value. A critical macroscopic strain γ_c of order of a few 10^{-2}% means that, at a local scale, the relative movement δ of two neighboring cement particles is reversible as long as it is inferior to $\gamma_c d \approx$ a few nm where $d \approx 10\,\mu m$ is the typical size of a cement particle. This would mean that there are some links of size of the order of a few nm between the cement particles that are broken for strains higher than the first critical macroscopic strain.

Confirmation of this first basic interpretation and a better insight on the nature of these links is gained from existing literature. The storage shear modulus measured below the lowest critical strain during the dormant period is actually usually seen to continuously increase in time [17,23]. This continuous increase has previously been associated to the formation of hydrates by Lei and Struble [23] in the case of cement pastes and Nachbaur et al. [17] in the case of both tri-calcium silicate and cement pastes. These authors suggested that the evolutions of the system before setting are the signatures of the CSH nucleation during the dormant period. These CSH were described as forming "bridges" between cement particles. After what was described in the above papers as the first short term coagulation phase, a long term second phase in the evolution of the elastic shear modulus was called rigidification in Refs. [24,25].

Several important experimental facts from the above papers confirm these interpretations:

A) As we pointed out above, the breakage of an inter-particle bond such as CSH particles that has a range δ of a couple nm with respect to cement particles whose size d is of the order of 10 μm would give a macroscopic critical strain δ/d in the range of a few hundredths of %.
B) Pseudo contact zones between grains are preferential sites for nucleation. This can explain that, although the degree of hydration is close to zero, the consequences of the CSH nucleation are strong at a macroscopic level as they nucleate specifically in very crucial zones in the interacting particles network.
C) This critical strain is of the same order of magnitude as the critical strain for which cracks propagate in hardened concrete. It

is also, in the case of hardened concrete, the end of the elastic linear regime.

It has to be kept in mind that, in cement pastes, other early hydration products than CSH could nucleate and have macroscopic consequences on the rheological behavior. We will however in this paper follow the above authors and keep on assuming that the nucleating products at the origin of the rigidification process are CSH for the following reasons:

A) C_3S pastes in Ref. [17] had a similar rigidification behavior as standard cement pastes and CSH nucleation was sufficient to explain the measured behavior without any contribution from any other hydration products.
B) Most other potential hydration products are far bigger than a few nm and cannot therefore nucleate in the pseudo-contact zones between flocculated cement particles in which the separating distance between cement grains surfaces is of the order of a few nm [26]. Nucleation at any other locations in the system, as long as the volume fraction of the nucleated products remains low, shall not have any major consequences on the rheological behavior of the system.
C) All measurements in this paper are carried out at least 20 min after mixing. The early hydration reactions have already occurred in the system. Their consequences in terms of cement particles interactions are erased by the strong pre-shearing described above before each test. Because of this specific procedure, no structural breakdown may be spotted [1].

Finally, this leads to interpreting the first critical strain as a signature of the breaking of CSH links between cement particles. In order to simplify our text in the following, we will from now on call the smallest critical strain, below which very high values of the storage modulus are measured, the *rigid critical strain* in opposition to the soft *colloidal critical strain* described below. It will however be necessary to keep in mind that, at the nano-scale, CSH bridges can also be seen as dense suspensions of particles, the cohesion of which originates from colloidal forces (*i.e.* ion correlation forces) [27,28]

2.3. The largest critical strain: the colloidal contribution

While a low critical strain had to be associated with short range links between the particles, a large critical strain certainly involves non-contact interactions between the particles: it implies rather large movement of two neighboring cement particles. This is consistent with the critical strain above which the particle start to rearrange and flow starts in many other colloidal suspensions in nature or industry [12,13,20] where only such interactions are involved.

Several types of non-contact interactions occur within a cementitious suspension [10]. At short distance, cement particles interact via (generally attractive) van der Waals forces [26]. Also, there are electrostatic forces that result from the presence of adsorbed ions at the surface of the particles [29]. Polymer additives (such as High Range Water Reducing Admixtures HRWRA), present in many modern cementitious materials, can induce steric hindrance [30–32], which is believed to predominate over electrostatic repulsion. Each of these different interactions introduces non-contact forces between particles, the magnitude of which depend primarily on their separation distance. Repulsive electrostatic forces alone are generally insufficient to prevent agglomeration due to van der Waals attractive forces and steric hindrance or additional electrostatic repulsion from polymers is needed to disperse cement particles.

Due to the high particle volume fraction of cement pastes, there exists in the material a percolated network of particle–particle colloidal attractive interactions, which allows the suspension to support finite amount of stress without flowing. This network breakage occurs when its initial shape has been sufficiently modified, namely for a critical strain γ_c of order of a few % as observed in Fig. 2a.

3. Kinetics of percolation(s) and rigidification

In the previous section, we have shown that two critical strains, which can be related to CSH and colloidal links between cement particles, exist in a given cement paste. In order to get a better insight in the macroscopic structuration of cement pastes and of its origin, we now use elastic modulus measurements with oscillation to characterize the structuration kinetics associated with both kinds of interactions between cement particles.

3.1. Macroscopic observations

3.1.1. Independent macroscopic measurements of the two structuration kinetics

In order to study independently the formation of the two networks, we apply oscillating strains of different amplitudes and frequencies.

First, in order to measure the kinetics of the rigid interactions network evolution, we simply apply oscillations of amplitude lower than the rigid critical strain as in Refs. [17,18]. As, below the rigid critical strain, the answer of the system is purely elastic, the measured stress is in phase with applied oscillating strain as shown in Fig. 4 and the storage elastic modulus is equal to the instantaneous shear elastic modulus of the system.

We measured the evolution of this modulus in the case of our cement paste. 20 min after mixing, we pre-sheared the paste at 150 s^{-1} for 150 s. Straight after pre-shear, we applied an oscillating strain of amplitude 0.03% at a 1 Hz frequency. After a few hundred seconds, the evolution of the elastic modulus becomes linear with time as shown in Fig. 5, as already measured in Ref. [17].

In order to study the kinetics of formation of the colloidal network, we should apply oscillations of amplitude larger than the rigid critical deformation (*i.e.* 0.5%). Such a deformation is indeed large enough to break the CSH bridges formed between cement particles. This is however not sufficient as discussed below.

In Fig. 6, the relative amplitude of applied oscillating strain (*i.e.* the ratio between the applied strain and the strain amplitude) and the relative amplitude of measured stress (*i.e.* the ratio between the measured stress and the stress amplitude) are plotted as a function of time during a couple of oscillation periods at 1 Hz for an amplitude of 0.5%. The cement paste, the measurement protocol and the Vane

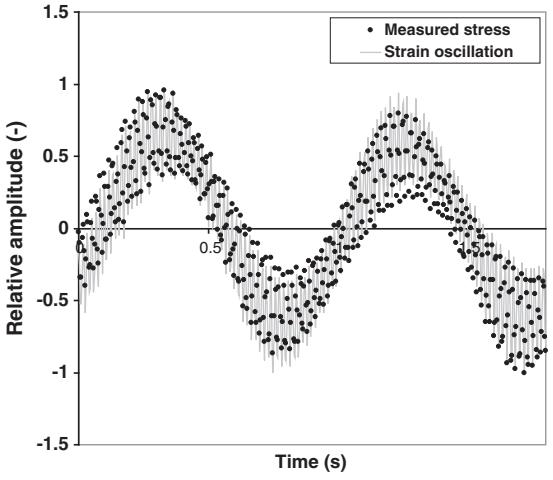

Fig. 4. Relative amplitudes of applied strain and measured stress as a function of time. The amplitude of the strain oscillation is 0.05% and the frequency is 1 Hz.

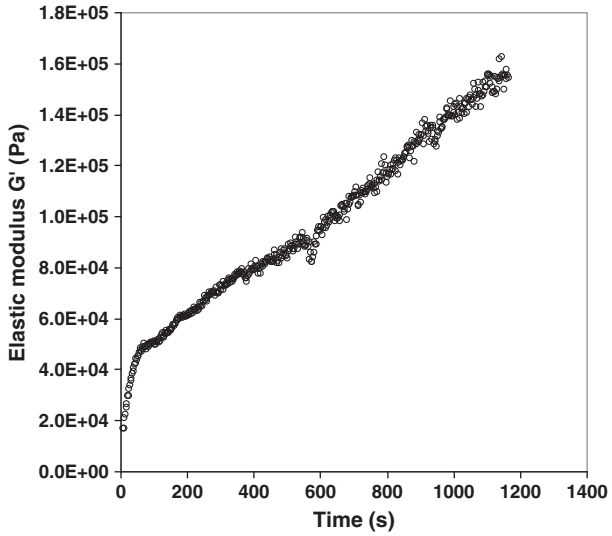

Fig. 5. Evolution of the elastic modulus of the rigid network as a function of time. Strain amplitude 0.0003, frequency 1 Hz.

tool are the same as the ones described previously in this paper. There is no resting time before test starts.

Let us comment on Fig. 6. We start at the peak of the strain oscillation, when the oscillating shear rate is equal to zero ($t \approx 0.3$ s). Then, during a very short time, the system is not sheared and can be considered as the reference initial configuration of the system. In this initial unsheared configuration, CSH nucleates between cement particles (*i.e.* in less than a couple tenths of seconds). As a consequence, from the point of view of these CSH, the system strain is zero and this can be considered as their elastic reference state. As the shear rate increases (t between 0.3 s and 0.4 s), the shear strain increases until it reaches the rigid critical strain (taking the initial configuration at $t \approx 0.3$ s as the reference configuration). Note that, during this period, the relative slope between stress and strain is very high showing how rigid the system is. At $t \approx 0.4$ s, the strain in the system at the scale of the CSH is of the order of one tenth of the strain amplitude (namely a strain of order 0.05%) and the CSH network breaks. Suddenly, the relative slope between stress and strain strongly decreases from 0.4 to 0.6 s. From 0.6 s, we suggest that most CSH have been destroyed and that the measured stress is now dictated mainly by the residual soft colloidal network (and potentially by an equilibrium between nucleation of CSH and their instantaneous destruction). The answer of this residual network is elastic as shown by the period during which both stress and strain are in phase (t between 0.6 s and 0.75 s). When $t \approx 0.75$ s, the oscillating shear rate reaches zero. Once again, it can be considered that, during a very short time, the system is not sheared and, again, CSH nucleates between cement particles, recreating a rigid interaction network, which will also be broken by the following relative increase in strain. It can be seen in Fig. 6 that the answer of the system is very complex: the system can be considered as visco-elasto-plastic, it can display two very different elasticities and, whereas the reference configuration shall be for zero strain, it is, at the scale of the nucleating CSH, reached every period as soon as the shear rate becomes too small to destroy them, *i.e.* at the peaks of the strain signal. Because of this complexity, some features are therefore difficult to explain: for instance, between 0.75 s and 0.8 s, although the strain is still increasing, the measured stress is decreasing. The value of the storage modulus measured using such oscillations is therefore very difficult to analyze and is strongly affected by the equilibrium between formation and destruction of the CSH bridges between particles.

In order to isolate the colloidal network, we therefore not only need to apply an oscillating strain larger than the rigid critical strain in order to destroy the CSH but we also should apply it at a frequency sufficiently high to reduce the influence of the CSH nucleation when the system reaches a zero strain rate configuration. In order to identify this frequency, we plot in Fig. 7 the complex modulus as function of the frequency for strain oscillations of amplitude 0.5%. We use the same test as above and test starts immediately after the pre-shear phase.

In a first regime (below 0.2 Hz), there is no steady state. The complex modulus keeps on increasing and no equilibrium between destruction and nucleation of CSH is reached. In a second regime, between 0.2 Hz and 5 Hz, a steady state is reached. It however depends on the frequency showing that CSH contributes to the measured stress and therefore to the computed complex modulus. As frequency increases, the role of CSH in the system decreases as the time during which they can nucleate shortens. In the last regime (above 5 Hz), the complex modulus does not depend on frequency. We can assume that, in this last regime, the oscillations are sufficiently large and fast to destroy all CSH, and that the time spent at rest (zero shear rate) is too short to allow new CSH bonds to form. It thus allows us to isolate the colloidal interactions network. With this procedure, the measured answer of the system is therefore dominated by the elastic answer of

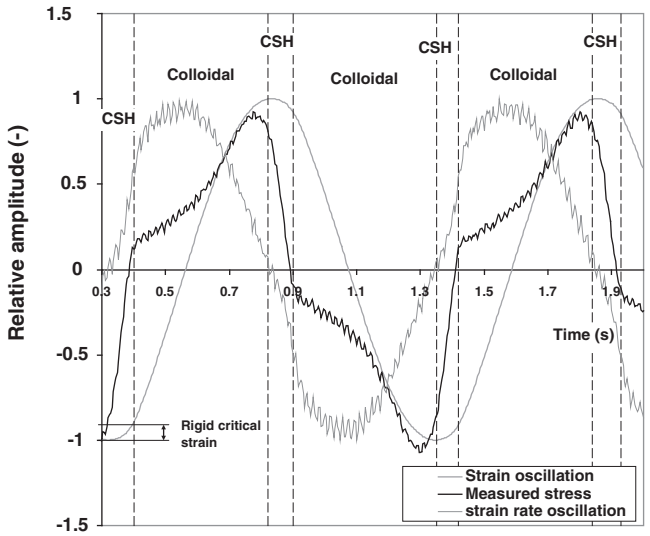

Fig. 6. Relative amplitudes of applied strain and measured stress as a function of time. The amplitude of the strain oscillation is 0.5%.

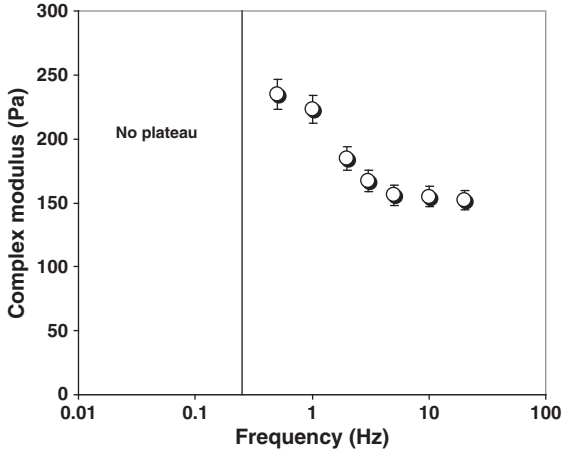

Fig. 7. Measured complex modulus in steady state as a function of oscillation frequency.

the colloidal network. By applying such strain oscillations, it is then possible to study independently the kinetic of the colloidal network formation. Using this type of oscillation, we measure the evolution of the storage or elastic modulus with time as plotted in Fig. 8. 20 min after mixing, the same cement paste as above (W/C = 0.4) is pre-sheared at 150 s^{-1} for 200 s. The oscillations are applied straight after the end of the pre-shear at a frequency of 10 Hz. It may be interesting to note that, in this regime, the storage modulus is lower than the viscous modulus and the system is only weakly elastic. The answer of the system at these high frequencies is indeed dominated by the viscous contribution of the sheared interstitial fluid. We focus now on the time needed to create this network. We can see in Fig. 8 that the elastic modulus increases during the first 10 s and then reaches a plateau. This means that, after 10 s, the network is formed and does not evolve anymore. The colloidal percolation characteristic time is therefore of the order of a few seconds.

3.2. Physical analysis

3.2.1. Colloidal percolation characteristic time

In many colloidal suspensions in nature or industry, coagulation or flocculation is dictated by the competition between Brownian motion that tends to bring the particles into contact and viscous effects, that dissipate the particle kinetic energy and slow the coagulation or flocculation process down. It was however shown in Ref. [11] that, in the case of standard cementitious systems with particles average diameter d being of the order of 10 μm, Brownian effects at short range are dominated by the attractive colloidal interactions described above. These attractive forces should replace, in the case of concentrated cement suspensions, Brownian motion as the origin of the flocculation. The process shall be slowed down by the viscous dissipation associated with the drag force exerted on particles by the suspending fluid (*i.e.* water in most cases), the viscosity of which is noted here μ_0.

In the particular case of nonretarded van der Waals interaction, which were shown to dominate the other colloidal interactions in the case of cement pastes and therefore dictate the inter-particle distance [31,33], Φ_0 is the energy potential and can be written as [34]:

$$\Phi_0 \cong \frac{A_0 a^*}{12H} \tag{1}$$

where a^* is the radius of curvature of the "contact" points, H is the surface to surface separation distance and A_0 is the Hamaker constant.

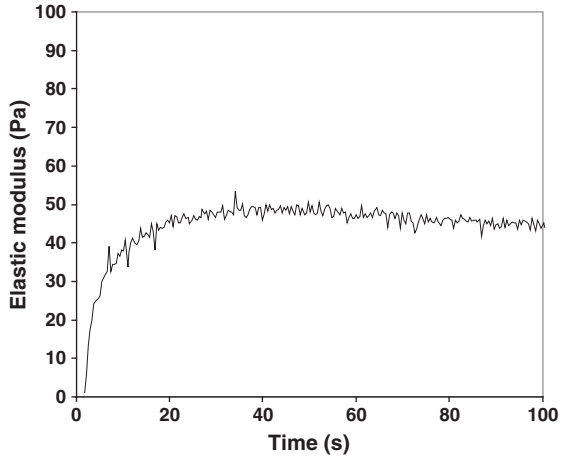

Fig. 8. Storage modulus as a function of time for our W/C = 0.35 cement paste. Frequency 10 Hz, amplitude 0.005.

Following the spirit of most coagulation theories [35–37] and assuming that cement grains can be described as mono-disperse particles, we introduce here the characteristic flocculation time $T_{flocculation}$:

$$T_{flocculation} = \frac{3\mu_0}{4N\Phi_0} \tag{2}$$

with N the total number of cement particles per unit volume. We first assume that the order of magnitude of the inter-particle distance to be accounted in Eq. (2) is not the average inter-particle distance of the order of 1 μm. We expect that, in such a dense system, it should be very easy to create a percolation path. The first percolation path appearing in the system shall therefore only involve particles, which were already almost in contact before flow stops. We thus assume that the order of magnitude of the inter-particle distance to be considered in the computation of the energy potential Φ_0 is the surface to surface distance at the "pseudo" contacts points in the flocculated system.

Let us now try to evaluate the value of this characteristic flocculation time. The values of H that may be found in literature are of the order of a few nm [26,31,38], consistently with the value of the rigid critical strain. The Hamaker constant value for C_3S is of the order of $1.6\,10^{-20}$ J [34]. The estimated value of a^* for cement particles is estimated to be of the order of a few hundred nm [11]. We consider here that the volume fraction ϕ of a standard cement paste is of the order of 40% with $\phi = (1 + \rho_p W/\rho_w C)^{-1}$ where ρ_p and ρ_w are respectively the density of the cement grains and the density of water. The number of cement particles per unit volume may be roughly estimated as ϕd^{-3}. The Newtonian viscosity of water μ_0 is of the order of 10^{-3} Pa.s at room temperature. Using the above values, it is found that the characteristic flocculation time is of the order of a couple of seconds.

The above analysis and the results from Fig. 8 show that, for most cementitious systems, colloidal percolation (*i.e.* the situation in which the network formed by the flocculated particles is strong enough to resist stress) should occur in the first seconds following beginning of rest.

3.2.2. From colloidal and rigid percolations to rigidification

The result obtained in the previous section is not in agreement with Ref. [17] in which it was concluded that the time needed after the end of mixing to form a coagulated network of particles was of the order of a few minutes. It has however to be kept in mind that the strain oscillations amplitude in Ref. [17] was 0.03%. As described in Section 3.1, this type of measurement is more representative of the consequences of the CSH nucleation than of the colloidal network evolution. It can therefore be concluded that the initial evolution in the material behavior measured during the first few minutes after the end of flow in Ref. [17] for very small strain amplitudes was not linked to colloidal flocculation and percolation but to CSH nucleation. It can moreover be concluded from the previous section that the initial evolution in the material behavior studied in Ref. [17] was in fact taking place in an already percolated colloidal network of cement particles.

We suggest here that there exists, after the colloidal network percolation, a transient phase, which finds its origin in the CSH nucleation. During this transient phase (that we will call here rigid percolation phase), the CSH nucleation turns locally the soft colloidal interaction between cement particles into a far more rigid interaction (*i.e.* higher energy potential), until a percolated network of cement particles with rigid interactions exist. In a second phase (that we will call here rigidification phase), when all soft interactions have been turned into rigid interactions, the continuing nucleation of CSH increases the rigidity by increasing either the number of bridges between particles or by increasing the size of the bridges.

Considering all the above, the following scheme can then be used to describe both short, medium and long term evolutions of fresh cement pastes [24,39] at rest during the dormant period:

- At the end of mixing phase, cement particles are dispersed (Fig. 9(a)).
- Because of colloidal attractive forces, cement particles flocculate in a few seconds and form a network of interacting particles able to resist stress and displaying an elastic modulus (Fig. 9(b)).
- Simultaneously, at the pseudo contact points between particles within the network, nucleation of CSH occurs although the material is still in the dormant period. This nucleation turns locally the soft colloidal interactions between cement particles into CSH bridges. As a consequence, at the macroscopic scale, the elastic modulus increases. After several tens of seconds (*e.g.* 100 s in Ref. [17], and 30 s here, see below), a percolation path of particles interacting purely through CSH bridges appears (Fig. 9(c)).
- Further increase of the macroscopic elastic modulus comes from an increase of the size or numbers of CSH bridges between percolated cement particles (Fig. 9(d)).

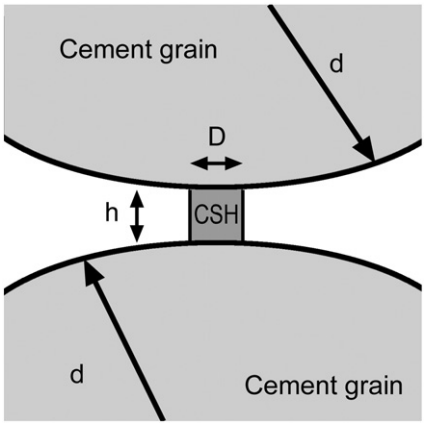

Fig. 10. CSH bridge between two cement grains.

3.2.3. Kinetics of rigidification

In order to go further in the analysis, we consider now a percolation path in the cement particles network (*i.e.* a succession of interacting cement particles able to transfer a macroscopic stress lower than the yield stress while keeping their respective positions). After the rigid percolation phase, this percolation path can be seen as a succession of cement particles interacting via rigid interactions due to CSH nucleation in the pseudo contact zones between these particles.

We assume that the bridges formed by the CSH between these cement grains can be considered as cylindrical homogeneous links of length H (the inter-particle distance) and of diameter D (see Fig. 10). We will consider in the following that both H and D are of the order of a couple nanometers whereas the diameter of the cement grains d is of the order of 10 μm. The elastic modulus G'_{CSH} of the CSH forming the link can be found in literature and is of the order of a few tens of GPa [40].

From the simple geometry shown in Fig. 10, it is first possible to show that, when a macroscopic stress is applied to the system, because of geometry effects, the stress concentrates in the CSH bridge. As a first approximation, it is possible to write that the macroscopic stress τ_{macro} applied to the percolated network and the local stress in the CSH bridge τ_{CSH} are related by $\tau_{macro}d^2 \approx \tau_{CSH}D^2$. The stress in the CSH bridge is therefore 10^8 times higher than the macroscopic stress.

Strain also concentrates in the CSH bridge. This local strain can be estimated as being $d/H \approx 10^4$ times higher than the macroscopic strain γ_{macro}. Therefore, when the rigid critical strain of order 10^{-2}% is applied to the system, the local CSH strain is of order 100%. This can be considered as an unusually high value for the fracture strain of rigid mineral solids but it is a standard order of magnitude for a dense suspension of elongated colloidal particles such as CSH pellets [40].

Keeping in mind that $\tau_{macro} = G'_{macro}\gamma_{macro}$ and $\tau_{CSH} = G'_{CSH}\gamma_{CSH}$, it is possible to write that $G'_{macro} = G'_{CSH}D^2/dH$. We then expect from this relation a macroscopic elastic modulus after the rigid percolation phase 10^4 times lower than the elastic modulus of the CSH, *i.e.* of the order of 1 MPa. This is not far from the values shown in Figs. 3 and 5 and close to the values obtained in Ref. [17]. It can be noted that, in order to get more quantitative values of this modulus, one would need to know the exact typology of the percolated network and use micromechanical models taking into account the exact geometry of the percolated path under consideration. This is however far beyond the scope of this paper.

Having checked the global consistency of our assumptions, we can now go further. We assume that the ongoing CSH nucleation increases the cross section of the CSH bridges.

As the heat of hydration, after the initial peak, is constant in the so-called "dormant" phase, it is possible to assume that the volume of hydrates at the contact points increases linearly with time. As the inter-particle distance H is fixed (*i.e.* the cement particles network spatial configuration stays unchanged [17]), D^2 increases linearly with time and the macroscopic elastic modulus of the cement paste (*i.e.* the strength of the cement particles network interacting through CSH bridges) $G'_{macro} = G'_{CSH}D^2/dH$ should also increase linearly with time. This is the case in Fig. 5 after a few hundred seconds. This would mean that, within the above theoretical frame, the colloidal percolation phase ends a few seconds after the end of the last strong

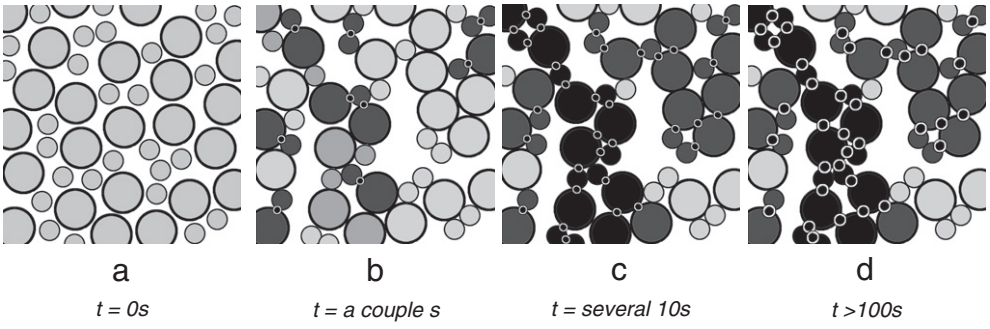

Fig. 9. Network(s) of interacting cement particles in the dormant period. All times are given as orders of magnitude. (a) Cement particles are dispersed at the end of the mixing phase; (b) A couple of seconds after the end of mixing, cement particles are flocculated forming a percolated network of colloidal interactions. Darker particles belong to a percolation path; at the pseudo contact points between particles, nucleation of CSH (black and white dots) starts immediately to turn locally the soft colloidal interaction between cement particles into a far more rigid interaction; (c) All the particles in the percolation path (black particles) are linked by CSH bridges forming a percolated rigid network in the material; (d) The elastic modulus of the mixture keeps on increasing as the size of the CSH bridges (black and white dots) increase.

shearing whereas the rigid percolation phase ends several hundreds of second later. From that point, the rigidification phase starts, during which the elastic modulus increases linearly with time.

4. Thixotropy and apparent yield stress

Thixotropy is a reversible macroscopic phenomenon and is therefore often associated to reversible physico-chemical phenomena such as flocculation and de-flocculation under shear of colloidal suspensions. It has however to be kept in mind that thixotropy is defined at a purely macroscopic level: it only implies that the macroscopic evolutions of the behavior of the material are reversible [3–9]. In the case of cement pastes, this means that, as long as shear is sufficient to bring the material back to a reference state, one does not have to care whether the evolution of the material behavior is due to colloidal flocculation or to CSH bridges between particles. Even if, at a microscopic scale, it is a nonreversible chemical reaction that creates bonds between particles, these may be weak enough to be broken by shear whereas new bonds may spontaneously appear again at rest [24,25] as long as the reservoir of chemical species is sufficient. Their formation is hence not incompatible with a macroscopic reversible evolution. From a practical point of view, hydration may therefore have reversible macroscopic consequences as long as the available mixing power is sufficient to break the CSH links between cement particles. Hydration is however at the origin of workability loss as soon as the available mixing power becomes insufficient to break these inter-particle connections [11,24,25], if we neglect here any chemical reactions between HRWRA and cement hydration [41].

We first check here that the thixotropic behavior of the W/C = 0.4 cement paste tested in this paper is fully reversible at high shear rates. 20 min after mixing, we first shear the paste at 150 s^{-1} for 150 s. We then leave it at rest for 5 min. In a third phase, we shear it again at 150 s^{-1} for 150 s. We then leave it at rest for 20 min. In a final phase, we shear it once again at 150 s^{-1} for 150 s. We use once again the same rheometer and Vane tool. We compute the apparent viscosity using a Couette analogy [42], assuming that, at these high shear rates, the gap is fully sheared. We plot in Fig. 11 the apparent viscosity (*i.e.* the ratio between shear stress and shear rate) of the paste.

In order to evidence the impact of hydration on the macroscopic reversible thixotropic behavior of a cement paste during the dormant period, we measure now the stress needed to initiate flow with our Vane tool after two resting times for our W/C = 0.4 cement paste at a shear rate of 0.005 s^{-1}. The results are plotted in Fig. 12.

We observe that, according to the resting time, the dominant peak stress will either be associated to the rupture of a soft colloidal network (*i.e.* for a 5 minute resting time, the stress peak occurs at a strain of the order of a few %) or to the rupture of a rigid CSH based network (*i.e.* at a longer resting time (20 min), the stress peak occurs at a strain of the order of a few hundredths of %). The stress peak at a 0.05% strain can be associated with the rigid network only (the contribution of the soft colloidal network to stress at such strain being negligible). It can also be seen that, although the soft critical strain does not change, the stress peak associated to the rupture of the colloidal network is increasing with the time at rest. As we have shown above in this paper that, after a few seconds, the colloidal network did not evolve anymore (the elastic modulus being constant), it can therefore be concluded that the stress associated to this peak is the result of the combination of soft colloidal interactions and CSH bridges between particles formed at rest that were not all broken when the rigid critical strain was reached or that continuously broke and reformed all along the measurement.

Other secondary comments can be made on Fig. 12. First, the strong fluctuations after the peak associated with the rupture of the rigid network at 20 min resting time are due to the rheometer, which is not able to keep on controlling accurately the strain rate during such an event. This illustrates the rigidity of this network, which breaks similarly to a fragile solid material.

Second, it can be seen in Fig. 12 that, contrary to Fig. 11, the material does not come back to the same reference state after the peak(s); this means that the yielding mechanism associated to the shear rate applied in this test (*i.e.* 0.005 s^{-1}) does not bring the system to a fully dispersed state but probably leads to residual flocs of cement particles of higher average size than the individual cement particles [43], and whose precise size depends on how yielding has occurred.

It can be concluded from Fig. 12 that, according to the resting time, the measured apparent yield stress in practice will be the first or the second peak. As it was demonstrated that the critical strain associated to the rigid contact interactions does not change much with time [17] (*i.e.* it stays of the order of few hundredths of %) and as we have shown above that the evolution of the rigid network elastic modulus associated to CSH nucleation is linear with time, the critical stress associated to the rupture of this network should also increase linearly with time. As soon as this critical stress is the dominant one, the measured yield stress should also increase linearly with time. This explains why, in literature, most measurements of apparent yield stresses on observation periods of the order of 1 h have shown linear evolution of the yield stress with time. This is also the case of the cement paste studied in this paper as shown in Fig. 13. We plot in this figure the highest peak stress measured through the same Vane test

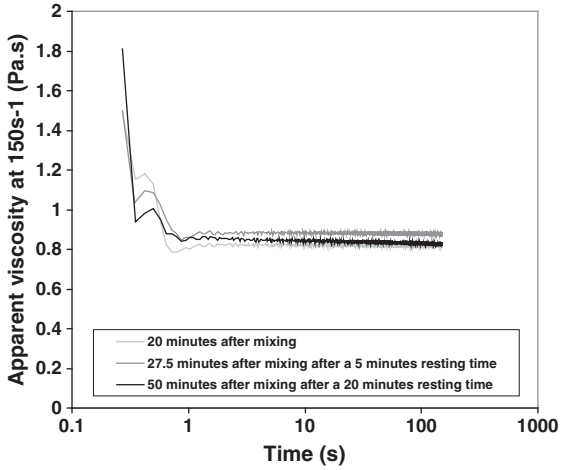

Fig. 11. Apparent viscosity as a function of time for the cement paste tested in this paper for successive shearings.

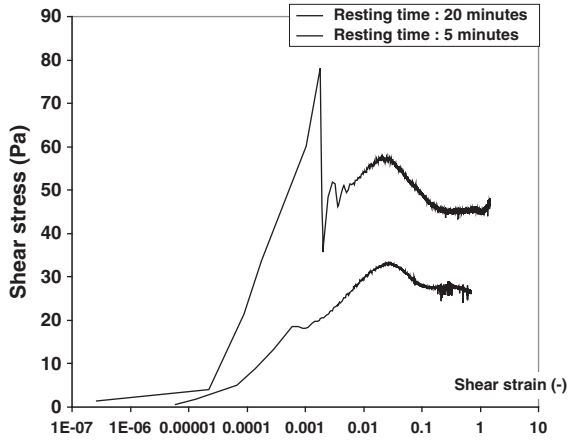

Fig. 12. Shear stress as a function of strain during a Vane test for a water to cement ratio of 0.4.

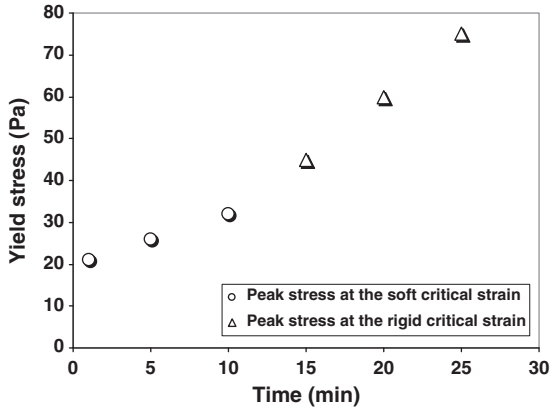

Fig. 13. Apparent or static yield stress as a function of resting time.

as above for various resting times. For resting times lower than 10 min, this peak stress is measured for the soft critical strain. For larger resting times, it is measured for the rigid critical strain. In the particular case of the pastes tested in this paper, this limit corresponds to the end of the rigid percolation phase.

It has finally to be kept in mind that what operators measure in most procedures and what matters in industrial practice is the value of the stress peak no matter its origin. Indeed, practical problems involving thixotropy include stability of coarse aggregates in cement paste, distinct-layers casting of SCC or formwork pressure prediction and are dictated by the evolution of the yield stress with time at rest at the scale of several tens of minutes [9]. However, as we have shown above that colloidal flocculation only affects thixotropy on a few seconds time scale and that even the evolution of the stress associated to the soft critical strain seems to be strongly affected by CSH nucleation, we suggest here that, in practice, thixotropy is mainly affected by CSH nucleation.

This explains why one of the most efficient ways to create very thixotropic concrete is to introduce hydration accelerating products in the mixture [44] or fine silica or limestone particles that will act as intercalated grains with strong nucleating properties. As soon as the mixing power available during industrial processes is sufficient to break the additional CSH bonds created by these products, they enhance thixotropy without any workability loss. The results obtained here also explain why temperature, which strongly affects the hydration chemical reaction, is also a strong thixotropy and sometimes workability loss enhancer [45].

5. Conclusion

We have first clarified in this paper the ambiguity in literature concerning the critical strain of fresh cement paste. Thanks to a detailed analysis of the macroscopic behavior of a paste, we have shown that there exist two critical strains. We attribute each of these critical strains to a specific physical and chemical phenomenon involved in the behavior of the paste in the fresh state.

The largest critical strain is of the order of a few % and can be associated to the network of colloidal interactions between cement particles. The time needed to form this network is of the order of a couple seconds.

The smallest critical strain is of the order of several hundredths of % and can be associated to the early hydrates, which form preferentially at the contact points between aggregated cement grains. It develops as soon as some particles are flocculated in the mixture. The development of the network of cement particles interacting via CSH bridges can be decomposed in two successive phases: a rigid percolation phase followed by a rigidification phase during which the elastic modulus at low strain increases linearly in time. These have reversible macroscopic consequences as long as the available mixing power is sufficient to break the rigid links between cement particles. It is however at the origin of workability loss as soon as the available mixing power becomes insufficient to break these inter-particle connections.

The value of the apparent yield stress of the mixture left at rest results from the two above phenomena. Depending on resting time, the dominant stress peak observed during a static yield stress measurement will be either measured for the rigid critical strain (at long times) or for the colloidal critical strain (at short times). At the rigid critical strain, its value is only determined by the strength of the CSH bonds in the rigid network. At the colloidal critical strain, its value is also affected by CSH nucleation. As we have shown here that the evolution of the elastic modulus of the rigid network is, in most cases, linear with time, the long term structural build up of the material which is associated with the rigid network only, is also linear in time as often measured in literature.

References

[1] G.H. Tatersall, P.G.F. Banfill, The Rheology of Fresh Concrete, Pitman, London, 1983.
[2] N. Roussel, Rheology of fresh concrete: from measurements to predictions of casting processes, Mater. Struct. 40 (10) (2007) 1001–1012.
[3] H.A. Barnes, Thixotropy — a review, J. Non-Newtonian Fluid Mech. 70 (1997) 1–33.
[4] R. Lapasin, V. Longo, S. Rajgelj, Thixotropic behaviour of cement pastes, Cem. Concr. Res. 9 (1979) 309–318.
[5] Y. Otsubo, S. Miyai, K. Umeya, Time-dependant flow of cement pastes, Cem. Concr. Res. 10 (1980) 631–638.
[6] P.F.G. Banfill, D.C. Saunders, On the viscosimetric examination of cement pastes, Cem. Concr. Res. 11 (1981) 363–370.
[7] A. Papo, The thixotropic behaviour of white Portland cement pastes, Cem. Concr. Res. 18 (1988) 595–603.
[8] N. Roussel, Steady and transient flow behaviour of fresh cement pastes, Cem. Concr. Res. 35(9) (2005) 1656–1664.
[9] N. Roussel, A thixotropy model for fresh fluid concretes: theory, validation and applications, Cem. Concr. Res. 36 (2006) 1797–1806.
[10] R.J. Flatt, Towards a prediction of superplasticized concrete rheology, Mater. Struct. 27 (2004) 289–300.
[11] N. Roussel, A. Lemaître, R.J. Flatt, P. Coussot, Steady state flow of cement suspensions: a micromechanical state of the art, Cem. Concr. Res. 40 (2010) 77–84.
[12] C.E. Maloney, A. Lemaitre, Amorphous systems in athermal, quasistatic shear, Phys. Rev. E 74 (2006) 016118.
[13] C.F. Zukoski, Particles and suspensions in chemical engineering: accomplishments and prospects, Chem. Eng. Sci. 50 (24) (1995) 4073–4079.
[14] S. Hutzler, D. Weaire, F. Bolton, The effects of Plateau borders in the two-dimensional soap froth III. Further results, Philos. Mag. B 71 (3) (1995) 277–289.
[15] F. Mahaut, S. Mokeddem, X. Chateau, N. Roussel, G. Ovarlez, Effect of coarse particle volume fraction on the yield stress and thixotropy of cementitious materials, Cem. Concr. Res. 38 (2008) 1276–1285.
[16] G. Schmidt, E. Schlegel, Rheological characterization of C-S-H phases-water suspensions, Cem. Concr. Res. 32 (2002) 593–599.
[17] L. Nachbaur, J.C. Mutin, A. Nonat, L. Choplin, Dynamic mode rheology of cement and tricalcium silicate pastes from mixing to setting, Cem. Concr. Res. 31 (2001) 183–192.
[18] M.A. Schultz, L. Struble, Use of oscillatory shear to study flow behavior of fresh cement paste, Cem. Concr. Res. 23 (1993) 273–282.
[19] P. Billberg, Form pressure generated by self-compacting concrete, Proceedings of the 3rd International RILEM Symposium on Self-Compacting Concrete, RILEM PRO33 Reykjavik, Iceland, 2003, pp. 271–280.
[20] C. Derec, G. Ducouret, A. Ajdari, F. Lequeux, Aging and nonlinear rheology in suspensions of polyethylene oxide-protected silica particles, Phys. Rev. E 67 (2003) 061403.
[21] T.G. Mason, J. Bibette, D.A. weitz, Yielding and flow of monodisperse emulsions, J. Colloid Interface Sci. 179 (1996) 439–448.
[22] R.J. Ketz, R.K. Prud'homme, W.W. Graessley, Rheology of concentrated microgel solutions, Rheol. Acta 27 (1988) 531–539.
[23] W.G. Lei, L.J. Struble, Microstructure and flow behavior of fresh cement paste, J. Am. Ceram. Soc. 80 (8) (1997) 2021–2028.
[24] S.P. Jiang, J.C. Mutin, A. Nonat, Studies on mechanisms and physico-chemical parameters at the origin of cement setting. 1. The fundamental processes involved during the cement setting, Cem. Concr. Res. 25(4) (1995) 779–789.
[25] A. Nonat, J.C. Mutin, X. Lecoq, S.P. Jiang, Physico-chemical parameters determining hydration and particle interactions during the setting of silicate cements, Solid State Ionics 101–103 (1997) 923–930.
[26] R.J. Flatt, Dispersion forces in cement suspensions, Cem. Concr. Res. 34 (2004) 399–408.

[27] R.J.-M. Pellenq, J.M. Caillol, A. Delville, Electrostatic attraction between two charged surface: a (N,V,T) Monte Carlo simulation, J. Phys. Chem. B 101 (1997) 8584–8594.
[28] S. Lesko, E. Lesniewska, An. Nonat, J.-C. Mutin, J.-P. Goudonnet, Investigation by atomic force microscopy of forces at the origin of cement cohesion, Ultramicroscopy 86 (2001) 11–21.
[29] R.J. Flatt, P. Bowen, Electrostatic repulsion between particles in cement suspensions: domain of validity of linearized Poisson–Boltzmann equation for non-ideal electrolytes, Cem. Concr. Res. 33 (2003) 781–791.
[30] P.F.G. Banfill, A discussion of the paper "Rheological properties of cement mixes", in: M. Daimon, D.M. Roy (Eds.), Cement and Concrete Research, Vol. 9, 1979, pp. 795–798.
[31] K. Yoshioka, E. Sakai, M. Daimon, A. Kitahar, Role of steric hindrance in the performance of superplasticizers in concrete, J. Am. Ceram. Soc. 80(10) (1997) 2667–2671.
[32] A. Zingg, L. Holzer, A. Kaech, F. Winnefeld, J. Pakusch, S. Becker, L. Gauckler, The microstructure of dispersed and non-dispersed fresh cement pastes — new insight by cryo-microscopy, Cem. Concr. Res. 38 (2008) 522–529.
[33] C.M. Neubauer, M. Yang, H.M. Jennings, Inter-particle potential and sedimentation behaviour of cement suspensions: effects of admixtures, Adv. Cem. Based Mater. 8 (1998) 17–27.
[34] R.J. Flatt, P. Bowen, Yodel: a yield stress model for suspensions, J. Am. Ceram. Soc. 89 (4) (2006) 1244–1256.
[35] Tomonori Fukasawa, Yasuhisa Adachi, Effect of floc structure on the rate of Brownian coagulation, J. Colloid Interface Sci. 304 (2006) 115–118.
[36] L.S. Tawari, D.L. Koch, C. Cohen, Electrical double-layer effects on the Brownian diffusivity and aggregation rate of laponite clay particles, J. Colloid Interface Sci. 240 (2001) 54–66.
[37] J.L. Baldwin, B.A. Dempsey, Effects of Brownian motion and structured water on aggregation of charged particles, Colloids Surf., A 177 (2001) 111–122.
[38] A.M. Kjeldsen, R.J. Flatt, L. Bergström, Relating the molecular structure of comb-type superplasticizers to the compression rheology of MgO suspensions, Cem. Concr. Res. 36 (2006) 1231–1239.
[39] Platel, D., The impact of the polymer architecture on the physico-chemistry properties of cement slurries. PhD thesis, ESPCI, Paris, (2005).
[40] M. Van Damme, The nanogranular origin of concrete creep: a nanoindentation investigation of microstructure and fundamental properties of calcium-silicate-hydrates, Thesis, MIT, Cambridge.
[41] R.J. Flatt, Y.F. Houst, A simplified view on chemical effects perturbing the action of superplasticizers, Cem. Concr. Res. 31 (2001) 1169–1176.
[42] P. Estellé, C. Lanos, A. Perrot, S. Amziane, Processing the vane shear flow data from Couette analogy, Appl. Rheol. 18 (2008) 34037–34481.
[43] K. Masschaele, J. Fransaer, J. Vermant, Direct visualization of yielding in model two-dimensional colloidal gels subjected to shear flow, J. Rheol. 53(6) (2009) 1437–1460.
[44] N. Roussel, F. Cussigh, Distinct-layer casting of SCC: the mechanical consequences of thixotropy, Cem. Concr. Res. 38 (2008) 624–632.
[45] J.Y. Petit, K.H. Khayat, E. Wirquin, Coupled effect of time and temperature on variations of yield value of highly flowable mortar, Cem. Concr. Res. 36 (2006) 832–841.